[RESTRICTED]

Transactions of the Korean Nuclear Society Autumn Meeting
Gyeongju, Korea, October 29-30, 2026

Turbine-Side Load-Following Performance and Steam-Bypass Dependence of a MSR without Control-Drum Actuation

Sang-Jin Kim*, Woon-Ho Jeong, Hyun-Woong Lee, Ji-Hwan Kim (HDEC)
Hyundai Engineering & Construction, 75, Yulgok-ro, Jongno-gu, Seoul
** Corresponding author: sangjin@hdec.co.kr*

***Keywords : Molten Salt Reactor (MSR), Load-Following Operation, Once Through Steam Generator, GAMMA+, Fuel Temperature Feedback.**

1. Introduction

As the penetration of variable renewable energy sources increases, nuclear power plants are increasingly expected to provide flexible operation in addition to conventional baseload generation. In light-water reactors, load-following operation is generally achieved through coordinated control of the reactor and power-conversion systems. Liquid-fueled molten salt reactors (MSRs), in contrast, may adjust their thermal power through fuel-temperature and density reactivity feedback. Nevertheless, the reactor, circulating fuel-salt system, intermediate heat-transport system, steam generator, and power-conversion system remain strongly coupled. Therefore, the load-following characteristics of an MSR should be evaluated at the integrated system level.

Singh et al. developed a nonlinear dynamic model of a molten salt demonstration reactor coupled to a once-through steam generator and showed that the reactor could respond stably to feedwater-flow variations through temperature-based reactivity feedback without direct operator intervention [1]. Chen et al. investigated step, ramp, and daily load-following transients of a liquid-fueled MSR using a RELAP5/MOD4.0 model equipped with power- and temperature-control systems [2]. More recently, Lee et al. performed a preliminary GAMMA+ analysis of a 100-20-100% load-following transient using a reactor regulating system and active control-element motion [3]. In that study, the power-conversion system was represented as a boundary condition, and incorporation of more detailed power-conversion-system dynamics was identified as future work.

An important distinction in evaluating these systems is that accurate tracking of a turbine-side demand signal does not necessarily imply an equivalent reduction in reactor thermal power. If the reactor produces more thermal power than the turbine-side boundary accepts, a steam-bypass path may maintain the requested turbine-side duty and steam pressure by diverting the excess energy. Apparent load-following performance may therefore depend on the availability, capacity, and allowable operating duration of the bypass system.

In the present study, a 100-50-100% demand transient was analyzed using a GAMMA+ based integrated model of a 100-MWth chloride-fueled MSR. Unlike active reactor-power control strategies, the control-drum reactivity command was fixed at zero throughout the transient. Instead, the coolant-salt pump, feedwater system, turbine-side steam-flow boundary, and high-pressure steam bypass were coordinately controlled.

In this paper, the term *load demand* denotes the requested turbine-side thermal duty expressed as a percentage of the rated reactor thermal power. It does not denote the actual reactor thermal power or electrical generator output.

The study addresses two related questions: whether the coordinated control architecture can maintain the prescribed turbine-side thermal demand and steam conditions without control-drum actuation, and what sustained bypass duty is associated with that performance. The objectives are to:

1. quantify turbine-side thermal-demand tracking under zero control-drum actuation
2. evaluate the regulation of steam pressure, steam temperature, and average fuel-salt temperature
3. quantify the reactor-to-turbine thermal-power mismatch and the associated bypass flow, thermal duty, diverted steam mass, and cumulative bypassed energy
4. assess the operational implications of sustained steam-bypass operation during partial-load operation

Only the bypass-available control configuration is evaluated. Accordingly, the results establish the extent to which the implemented control solution relies on the bypass path, but they do not demonstrate that every alternative bypass-free control strategy would fail.

2. System Model and Analysis Method

2.1 Integrated System Model

The system-level thermal-hydraulic analysis was performed using GAMMA+. The reference system was a 100-MWth liquid-fueled MSR consisting of three coupled fluid systems:

- a fuel-salt system
- an intermediate coolant-salt system

[Secure Minds, Secure Finds] 본 문서는 현대건설㈜의 정보자산이므로 무단 전재 및 복제할 수 없으며, 이를 위반할 시에는 당사 사규 및 관련 법규에 의해 제재를 받을 수 있습니다.

- a water–steam system

The fuel salt was represented using a NaCl-KCl-UCl_3 based property model, whereas the intermediate coolant salt was represented using a NaCl-KCl-$MgCl_2$ based property model. The fuel-salt system consisted of the reactor vessel, two symmetric primary loops, two fuel-salt pumps, and two fuel-salt-to-coolant-salt heat exchangers. The intermediate system included the coolant-salt side of the heat exchangers, a common hot leg, a coolant-salt pump, the salt side of the once-through steam generator, and an accumulator. The water-steam system provided the feedwater inlet and separate turbine-side and steam-bypass flow boundaries.

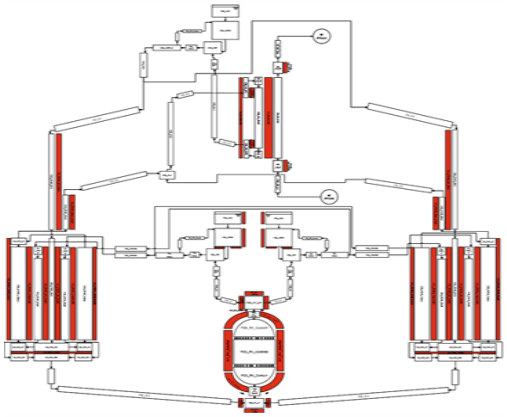


Fig 1. Nodalization of Integrated Reactor, Fuel salt, Coolant salt, Steam Generator, TV/BP system

Table 1. Principal model parameters and boundary conditions

Parameter	Value
Rated reactor thermal power	100 MWth
Feedwater inlet condition	10.5 MPa, 300°C
Reference steam pressure	10.0 MPa
Reference steam temperature	522°C
Reference for average fuel-salt temperature	853.28 K

Reactor power was calculated using a six-group delayed-neutron point-kinetics model. The neutron generation time was set to 2.4×10^{-4} s, and decay heat was calculated using the ANS-79 model. No load-following reactivity command was introduced through control-rod or control-drum motion. The reactor-power response was therefore governed by the modeled reactivity feedback, principally the fuel-temperature contribution, together with the thermal response of the heat-removal systems.

2.2 Coordinated Control Strategy

The load demand, L(t), was expressed as a percentage of the rated thermal power. The average fuel-salt temperature was calculated from representative hot-leg and cold-leg temperatures:

$$\overline{T_f} = \frac{T_{f,h} + T_{f,c}}{2}$$

where $T_{f,h}$ and $T_{f,c}$ are the representative fuel-salt hot- and cold-leg temperatures, respectively.

The coolant-salt pump command consisted of load feedforward and average fuel-salt temperature feedback:

$$u_{CSP} = sat_{30}^{110}\left[1.2L + 0.20\left(\overline{T_f} - 853.28\right) - 20\right]$$

where u_{CSP} is the coolant-salt pump command in percent and sat_a^b denotes saturation between the lower limit a and upper limit b. A 100% command corresponded to a mass flow rate of 1,079 kg/s. The pump response was represented by a first-order lag with a time constant of 60 s.

The feedwater controller consisted of demand feedforward, proportional-integral steam-temperature control, and a low-pressure correction term:

$$u_{FW} = sat_{10}^{100}\left[L + 3.0e_T + 0.03\int e_T dt + u_P\right]$$
$$e_T = T_s - 795.15$$

where T_s is the steam-generator outlet temperature in K and u_P is the low-pressure correction signal. A 100% feedwater command corresponded to 47.84 kg/s, and a first-order lag with a 45-s time constant was applied.

The turbine-side steam-flow command was determined from the load demand and steam-pressure deviation:

$$u_{TV} = sat_0^{100}[L + 10(P_s - 10.0)]$$

where P_s is the steam-generator outlet pressure in MPa. The turbine-side flow response was represented using a 30-s time constant.

The steam bypass was activated only when the steam pressure exceeded 10.01 MPa:

$$u_{BP} = sat_0^{100}[400\max(P_s - 10.01, 0)]$$

The bypass response was represented using a 10-s time constant. Both the turbine-side and bypass mass-flow boundaries had a rated flow of 47.84 kg/s.

The control-drum reactivity command remained fixed at zero during the complete transient. Thus, the actively controlled quantities were the coolant-salt pump flow,

[Secure Minds, Secure Finds] 본 문서는 현대건설㈜의 정보자산이므로 무단 전재 및 복제할 수 없으며, 이를 위반할 시에는 당사 사규 및 관련 법규에 의해 제재를 받을 수 있습니다.

feedwater flow, turbine-side steam flow, and steam-bypass flow.

The turbine-side thermal power was calculated as

$$Q_{TV} = \frac{\dot{m}_{TV}(h_{SG,out} - h_{FW})}{10^6}$$

and the bypass thermal power was calculated as

$$Q_{BP} = \frac{\dot{m}_{BP}(h_{SG,out} - h_{FW})}{10^6}$$

where $\dot{m}_{TV}$ and $\dot{m}_{BP}$ are the turbine-side and bypass steam mass flow rates, respectively. The terms $h_{SG,out}$ and h_{FW} denote the steam-generator outlet and feedwater-inlet specific enthalpies.

Here, Q_{TV} and Q_{BP} are expressed in MWth. The calculated turbine-side power represents the thermal duty delivered to the turbine-side boundary rather than electrical generator output. Turbine efficiency, generator dynamics, and condenser behavior were not included in the model.

2.3 Load-Demand Scenario and Bypass Assumptions

The prescribed demand history consisted of four periods:

- 0–1,440 s: linear decrease from 100% to 50%
- 1,440–3,600 s: constant 50% demand
- 3,600–5,040 s: linear increase from 50% to 100%
- 5,040–7,200 s: constant 100% demand

The demand-change rates during the downward and upward ramps were -2.083 and +2.083 %/min, respectively. The total simulation duration was 7,200 s, and the principal output variables were recorded at approximately 1-s intervals.

The requested turbine-side thermal duty was defined as

$$Q_D(t) = \frac{L(t)}{100} Q_{rated}$$

where $Q_{rated} = 100\ MWth$. The turbine-side tracking error was evaluated as the difference between Q_{TV} and Q_D.

The steam bypass was modeled as a controlled mass-flow boundary rather than as a detailed physical valve and downstream condenser system. No additional restriction was imposed on continuous bypass duration or cumulative bypassed energy. The downstream boundary was assumed capable of accepting the commanded bypass flow and associated thermal duty throughout the transient.

Consequently, the analysis quantifies the bypass service required by the evaluated controller, but it does not establish equipment-level feasibility or the actual continuous-duty capability of the bypass valve, condenser, or downstream heat-rejection system. The reported control performance is therefore conditional on sustained bypass availability and adequate downstream heat-rejection capacity.

3. Results and Discussion

3.1 Turbine-Side Demand Following and Reactor-Power Response

Figures 2 and 3 compare the prescribed turbine-side demand with the reactor thermal power, the thermal power transferred to the turbine-side boundary, and the steam-bypass mass flow rate. The turbine-side thermal power closely followed the prescribed demand during both the downward and upward ramps.

Over the complete 7,200-s simulation, the maximum absolute turbine-side tracking error was approximately 0.447 MWth, and the mean absolute error was approximately 0.259 MWth.

During the latter part of the 50% turbine-side demand hold, the average turbine-side thermal power was approximately 50.43 MWth. The reactor thermal power, however, remained substantially higher at approximately 65.67 MWth. Immediately after completion of the downward ramp, the reactor power reached a minimum of approximately 64.81 MWth and subsequently approached a partial-load equilibrium near 65.7 MWth.

Thus, although the turbine-side boundary accurately followed the 50% demand command, the reactor itself did not reach 50% of its rated thermal power.

.

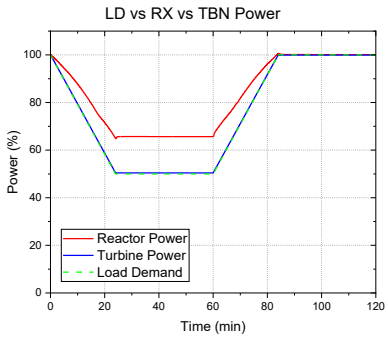


Fig 2. Load Demand, RX power, TBN power

[Secure Minds, Secure Finds] 본 문서는 현대건설㈜의 정보자산이므로 무단 전재 및 복제할 수 없으며, 이를 위반할 시에는 당사 사규 및 관련 법규에 의해 제재를 받을 수 있습니다.

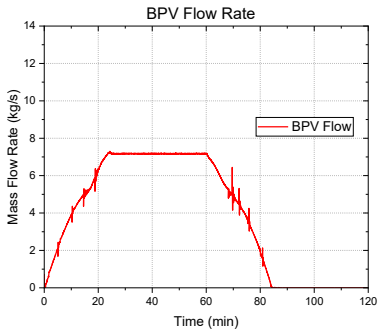


Fig 3. Bypass valve flow

At the 50% turbine-side demand condition, the turbine-side and bypass steam mass flow rates were approximately 24.15 and 7.18 kg/s, respectively. Their sum was approximately 31.33 kg/s, which was consistent with the feedwater mass flow rate and indicated satisfactory mass-flow closure across the steam generator.

The difference between the reactor thermal power and turbine-side thermal power was approximately 15.24 MWth. The estimated bypass thermal power was approximately 14.99 MWth. Consequently,

$$50.43 + 14.99 = 65.42\ MWth$$

which was close to the reactor thermal power of 65.67 MWth. The remaining difference of approximately 0.25 MWth can be attributed to changes in system thermal inventory, modeled heat losses, and numerical imbalance.

This thermal-power balance shows that the turbine-side demand was maintained near 50% by continuously diverting the reactor-to-turbine thermal-power mismatch through the steam-bypass path. The simulated response should therefore be classified as bypass-assisted turbine-side demand following rather than direct 50% reactor-power following.

3.2 Steam-Bypass Operation and Cumulative Thermal Energy

During the 50% turbine-side demand hold, the bypass flow accounted for approximately 22.9% of the total steam flow. The bypass remained continuously active during the 36-min hold period.

The maximum bypass flow over the complete transient was approximately 7.30 kg/s, corresponding to a maximum bypass thermal power of approximately 15.25 MWth. During the latter part of the 50% hold, the corresponding values were approximately 7.18 kg/s and 14.99 MWth.

The cumulative mass of steam diverted through the bypass over the complete 7,200-s transient was approximately 27.44 metric tons. Approximately 15.51 metric tons, or 56.5% of the total bypassed steam, occurred during the 50% turbine-side demand-hold period.

The cumulative bypassed thermal energy was approximately 15.92 MWhth. Over the same cycle, the integrated reactor thermal energy was approximately 166.85 MWhth, whereas approximately 150.40 MWhth was transferred to the turbine-side boundary. Thus, approximately 9.5% of the reactor-generated thermal energy was diverted through the bypass during the analyzed cycle.

The bypass therefore performed two functions. During the load ramps, it mitigated transient increases in steam pressure. During the extended partial-load period, it provided a sustained heat-removal path that separated the reactor thermal output from the lower turbine-side thermal demand.

This behavior supported steam-pressure regulation but introduced a non-negligible energy-utilization penalty. More importantly, the demonstrated partial-load operating point depended on the continued availability of a bypass path capable of accommodating approximately 15 MWth of excess thermal power.

3.3 Steam-Pressure and Steam-Temperature Regulation

Figures 4 and 5 show the steam-generator outlet pressure and temperature responses. The steam pressure remained between approximately 9.965 and 10.048 MPa throughout the transient. Relative to the reference pressure of 10 MPa, these values corresponded to deviations of approximately \(-0.35\%\) and \(+0.48\%\), respectively.

The mean pressure over the 50% turbine-side demand hold was approximately 10.0475 MPa. After the demand returned to 100%, the steam pressure approached approximately 9.997 MPa.

The steam-generator outlet temperature remained within approximately 520.7-522.8°C. During both the 50% and final 100% demand-hold periods, the temperature converged to approximately 522.0°C. The coordinated control system therefore maintained the steam pressure and temperature within bounded ranges during the evaluated transient.

[Secure Minds, Secure Finds] 본 문서는 현대건설㈜의 정보자산이므로 무단 전재 및 복제할 수 없으며, 이를 위반할 시에는 당사 사규 및 관련 법규에 의해 제재를 받을 수 있습니다.

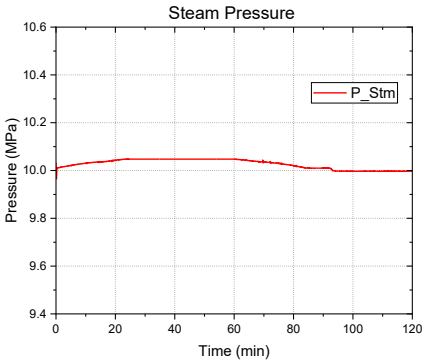


Fig 4. Steam Pressure

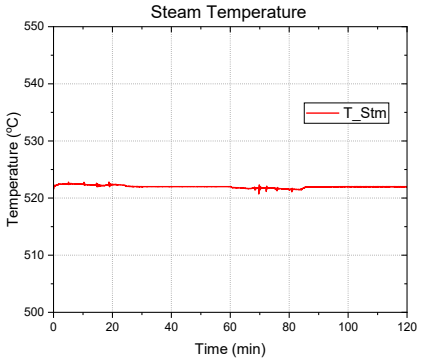


Fig 5. Steam Temperature

3.4 Thermal-Hydraulic State Associated with Sustained Bypass Operation

The thermal-hydraulic responses of the fuel-salt and coolant-salt systems were examined to characterize the partial-load equilibrium associated with the reactor-to-turbine thermal-power mismatch.

At the 50% turbine-side demand condition, the core fuel-salt flow rate remained close to its initial value of approximately 2,150 kg/s. The fuel-salt cold-leg temperature increased from approximately 541.0°C to 555.9°C, whereas the hot-leg temperature decreased from approximately 619.4°C to 607.1°C. Consequently, the fuel-salt temperature rise across the core decreased from approximately 78.3°C to 51.2°C.

Because the hot- and cold-leg temperatures changed in opposite directions, the average fuel-salt temperature changed by only approximately 1.3°C. The maximum absolute deviation of the average fuel-salt temperature from its reference value was approximately 1.44 K.

The fuel-salt response should therefore be described as convergence of the hot- and cold-leg temperatures at an approximately maintained average temperature rather than as a uniform decrease in fuel-salt temperature.

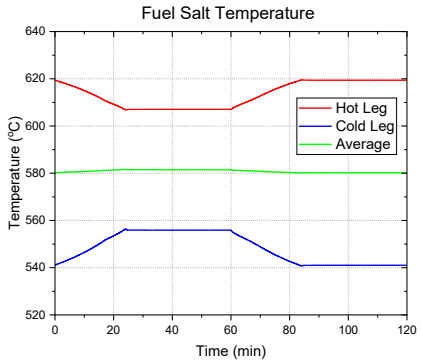


Fig 6. Fuel Salt Temperature

The intermediate coolant-salt system exhibited a different response. The coolant-salt flow rate through the steam generator decreased from approximately 962.5 kg/s to 384.2 kg/s, corresponding to approximately 39.9% of its initial value.

The coolant-salt cold-leg temperature decreased from approximately 455.8°C to 417.9°C, whereas the hot-leg temperature increased from approximately 551.3°C to 573.9°C. Consequently, the temperature difference across the coolant-salt system increased from approximately 95.5°C to 156.0°C.

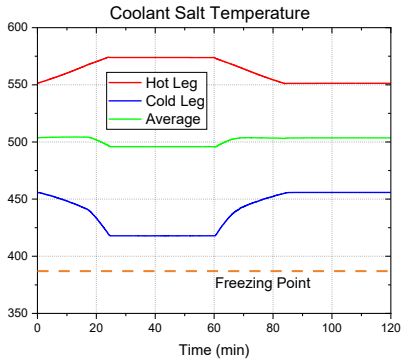


Fig 7. Coolant Salt Temperature

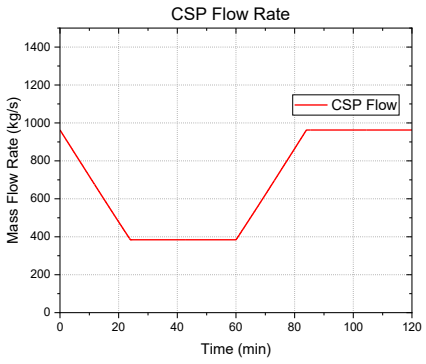


Fig 8. Coolant Salt Pump Flow

The two salt systems therefore exhibited distinct partial-load responses. The fuel-salt flow remained near

[Secure Minds, Secure Finds] 본 문서는 현대건설㈜의 정보자산이므로 무단 전재 및 복제할 수 없으며, 이를 위반할 시에는 당사 사규 및 관련 법규에 의해 제재를 받을 수 있습니다.

its rated value while its hot- and cold-leg temperatures converged. In contrast, the coolant-salt flow decreased to approximately 40% of its initial value while its temperature difference increased substantially.

Under the modeled controller settings and constant average fuel-salt-temperature reference, these coupled thermal-hydraulic responses established a reactor-power equilibrium near 65.7 MWth rather than at the turbine-side demand of approximately 50 MWth. The resulting thermal-power mismatch was accommodated by the steam-bypass path.

This result characterizes the equilibrium produced by the evaluated control configuration. It does not demonstrate that temperature feedback is intrinsically incapable of reaching a lower reactor-power level under a different temperature-reference schedule or control architecture.

3.5 Reactivity Feedback and Return to Full Load

All control-rod and control-drum command signals remained at zero throughout the transient. As shown in Figure 9, the calculated total reactivity varied from approximately -1.12 to +1.21 pcm, with the fuel-temperature reactivity term providing the principal contribution to the transient response.

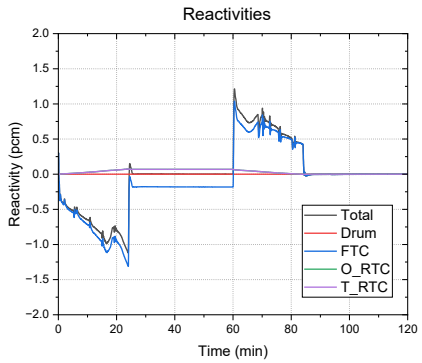


Fig 9. Reactivities

The relatively small total reactivity variation was consistent with the limited deviation of the average fuel-salt temperature from its reference value. It should not, however, be interpreted independently as proof that fuel-temperature feedback is fundamentally incapable of producing a larger reactor-power reduction.

The results instead show that, under the evaluated controller settings and thermal-hydraulic conditions, the feedback response produced a stable partial-load reactor power near 65.7 MWth.

After the turbine-side demand returned to 100%, the reactor thermal power approached approximately 100.14 MWth, while the turbine-side thermal power approached approximately 99.90 MWth. The principal fuel-salt and coolant-salt temperatures and flow rates also returned close to their initial values.

The fuel-salt accumulator levels, however, decreased from approximately 0.2737 m initially to 0.2381 m at the end of the transient, corresponding to a decrease of approximately 13%. Therefore, the observed near-recovery applies to reactor power and the selected thermal-hydraulic variables and should not be interpreted as complete recovery of every inventory-related system state or as confirmation of long-term cyclic repeatability.

3.6 Implications for Control-System Design

The coordinated control strategy maintained close turbine-side thermal-demand tracking and bounded steam conditions during the evaluated 100-50-100% transient without control-drum actuation. Its demonstrated partial-load performance, however, was conditional on sustained steam-bypass availability.

During the 50% turbine-side demand hold, the reactor remained near 65.7 MWth and approximately 15 MWth was continuously diverted through the bypass. The operating envelope represented by this calculation therefore included a bypass path and downstream heat sink capable of accepting a continuous flow of approximately 7.18 kg/s and a thermal duty of approximately 14.99 MWth, as well as peak values of approximately 7.30 kg/s and 15.25 MWth.

Accordingly, the present results support the following conditional conclusion: the controller can maintain the prescribed turbine-side thermal demand and steam conditions during the evaluated transient when sustained bypass operation of sufficient capacity is available and permitted.

If operating rules, equipment limitations, or downstream heat-rejection constraints prohibit such operation, the present calculation cannot be used to demonstrate acceptable 50% turbine-side demand operation. A different control configuration and separate validation would then be required.

Because a bypass-disabled or capacity-limited case was not analyzed, this study does not establish that every bypass-free control strategy would necessarily become unstable or fail to follow demand. Rather, it demonstrates that the implemented control configuration relied on sustained bypass operation to maintain the reported partial-load operating point.

Potential measures for reducing steady partial-load bypass dependence include:

- scheduling the average fuel-salt-temperature reference as a function of demand;

[Secure Minds, Secure Finds] 본 문서는 현대건설㈜의 정보자산이므로 무단 전재 및 복제할 수 없으며, 이를 위반할 시에는 당사 사규 및 관련 법규에 의해 제재를 받을 수 있습니다.

- introducing limited control-drum actuation or reactor-power-error feedback;
- optimizing the coolant-salt pump feedforward relationship;
- introducing an integral reactor-to-turbine power-mismatch signal through an appropriate actuator;
- coordinating the turbine-side and bypass pressure-control deadbands; and
- optimizing the controller gains and time constants.

Future comparative simulations should include bypass-disabled and bypass-capacity-limited cases, active reactor-power control, and alternative average-temperature reference schedules. Such calculations would establish whether acceptable operation can be achieved when continuous bypass service is unavailable or restricted.

4. Conclusions

A 100-50-100% turbine-side demand transient of a 100-MWth molten salt reactor was analyzed using a GAMMA+ based integrated system model with the control-drum command fixed at zero. The coordinated controller achieved close turbine-side demand tracking and maintained bounded steam pressure and temperature. However, the demonstrated performance represented bypass-assisted turbine-side demand following and was conditional on sustained steam-bypass availability during the partial-load hold.

The principal conclusions are as follows..

1. The turbine-side thermal power followed the prescribed demand with a maximum absolute error of approximately 0.447 MWth and a mean absolute error of approximately 0.259 MWth. The steam pressure remained within 9.965-10.048 MPa, and the steam-generator outlet temperature remained within approximately 520.7-522.8°C.

2. During the latter part of the 50% turbine-side demand hold, the reactor thermal power remained at approximately 65.67 MWth, whereas approximately 50.43 MWth was transferred to the turbine-side boundary. The resulting thermal-power mismatch was accommodated by a bypass flow of approximately 7.18 kg/s, corresponding to approximately 14.99 MWth and 22.9% of the total steam flow.

3. The cumulative bypassed thermal energy over the 7,200-s cycle was approximately 15.92 MWhth, equivalent to approximately 9.5% of the integrated reactor thermal energy. The bypass supported effective steam-pressure regulation but introduced an energy-utilization penalty and a requirement for continuous partial-load heat-rejection capability.

4. The average fuel-salt temperature remained close to its reference, with a maximum absolute deviation of approximately 1.44 K. Under the evaluated controller settings, the coupled thermal-hydraulic and reactivity responses established a reactor-power equilibrium near 65.7 MWth rather than at the 50% turbine-side demand.

5. Successful turbine-side demand tracking did not constitute equivalent reactor-power following. Within the evaluated configuration, the reported partial-load performance relied on sustained steam-bypass operation. The proposed strategy is therefore operationally applicable only within an operating envelope in which continuous bypass service of sufficient capacity and adequate downstream heat rejection are permitted and available.

The absence of a bypass-disabled or capacity-limited comparison prevents a universal conclusion that bypass-free operation would necessarily fail. Comparative analyses with alternative control settings are required to determine whether the observed bypass dependence can be reduced or eliminated.

ACKNOWLEDGMENT

This work was supported by the National Research Foundation of Korea (NRF), grant funded by the Korea government (MSIT) (RS-2023-00259713).

REFERENCES

[1] V. Singh, A. M. Wheeler, B. R. Upadhyaya, O. Chvála, and M. S. Greenwood, “Load-following operation and transient behavior of molten salt demonstration reactor,” Proceedings of the 11th Nuclear Plant Instrumentation, Control and Human-Machine Interface Technologies, American Nuclear Society, pp. 199–208, 2019.

[2] G. Chen, M. Li, Y. Zou, and H. Xu, “Analysis of load-following operation characteristics of liquid fuel molten salt reactor,” Progress in Nuclear Energy, Vol. 150, Article 104308, 2022.

[3] M. Lee, D. Yeo, T. Kim, Y. H. Yoo, B. Kim, and S. J. Kim, “A Preliminary Performance Analysis of Load-Following Capability in Molten Salt Reactor with Reactor Regulating System using GAMMA+,” *Transactions of the Korean Nuclear Society Autumn Meeting*, Changwon, Korea, Oct. 30–31, 2025.

[Secure Minds, Secure Finds] 본 문서는 현대건설㈜의 정보자산이므로 무단 전재 및 복제할 수 없으며, 이를 위반할 시에는 당사 사규 및 관련 법규에 의해 제재를 받을 수 있습니다.